Structural Analysis and Hydrogen Bonding Interactions on Pirimor and Water Mixture by Density Functional Theory

L.S. Anju, V.K. Suma, D. Aruldhas

Abstract-The geometrical parameters, different inter and intra molecular interactions of pirimor (PRM) and its water complex (PRM.3H_2O) have been performed using density functional theory (DFT) method with 6-31G(d) basis set. Charge analysis and Hirshfeld analysis reveals the charge transfer within the molecule. HOMO-LUMO energy gap, local softness and electrophlicity indices for selected atomic sites of the PRM and its water-complex were determined.

Key Words- Bioactivity, Hirshfeld analysis, Pirimor, Water mixture.

1. INTRODUCTION

Pyrimidine ring and its derivatives are known for their biological and pharmaceutical importance. Their properties are determined by hydrogen bonding and π – bonding systems. They belong to the family of nucleic acid. Pyrimidine and its derivatives have immense importance as antibiotics, and as crucial parts of many vitamins, and coenzymes. Pyrimidine-derived biomolecules have received much attention from spectroscopists, drug, clinical, and industrial researchers because of their therapeutic importance [1]. The present work gives a detailed structural analysis on Pirimor (PRM). It is used specifically to target insects and is applied as a foliar spray to infested plant material. The mode of action of Pirimor is that it inhibits acetylcholinesterase (AChE), thereby disrupting the neutral pathways of the insect. Pirimor is also found in formulation with many other insecticides. In this study, the structures of PRM.3H_2O complex formed by the hydrogen bonding interaction between PRM and three water molecules were studied. The energetic, vibrational frequencies of H-bonds were investigated. The natural bond orbital (NBO) analysis has been carried out to interpret hydrogen bonding, hyperconjugative interaction and intramolecular charge transfer (ICT). The calculated value of HOMO-LUMO energy gap is used to interpret the biological activity of the molecule [2]. Hydrogen bonding and hyperconjucative interactions have received much attention from both experimental and theoretical perspectives as they can determine the structures and biological activity of molecules.

- *L.S Anju- [a]Research Scholar, Register Number: 12049, Manonmaniam Sundaranar University, Abishekapatti, Tirunelveli - 627 012, Tamil Nadu, India. E-mail:anju.ls2007@gmail.com*
- *V.K. Suma- [a]Research Scholar, Register Number:11808, Manonmaniam Sundaranar University, Abishekapatti, Tirunelveli - 627 012, Tamil Nadu*
- *D.Aruldhas- [a, a*]Department of Physics& Research Centre, Nesamony Memorial Christian College, Marthandam 629 165, Tamilnadu, India.*

2. COMPUTATIONAL DETAILS

The structural analysis and spectroscopic studies of PRM and PRM.3H_2O were performed using Beck3-Lee-Yang-Parr (B3LYP) with 6-31G(d) basis set using GAUSSIAN 09 program package [3] without any constraint on the geometry. The optimized geometry corresponding to the minimum potential surface has been obtained by solving self-consistent field equation iteratively. The natural charges analysis interpret Atomic charges, donor-acceptor NBO hyperconjugative interactions, dipole moment, HOMO-LUMO energy gap were also computed [4]. Hirshfeld surface analysis of PRM has been constructed from CIF files in order to identify the interactions using crystal explorer 3.1[5].Gaussview.5.0.8 visualization program has been utilized to the shape of highest occupied molecular orbital (HOMO) and lowest unoccupied molecular orbital (LUMO).

3. RESULT AND DISCUSSION

3.1 OPTIMIZED GEOMETRY

The optimized geometrical parameters of Pirimor (PRM) and its water complex (PRM.3H_2O) were calculated by B3LYP with 6-31G(d) basis set. The results of the calculated geometrical parameters (bond length, bond angle and dihedral angle) are compared with the experimental values and are

listed in table 1. The optimized molecular structures with atom numbering scheme adopted in the computation is shown in fig.1

TABLE 1: STRUCTURAL PARAMETERS OF HYDROGEN BONDS IN PRM.3H_2O COMPLEX

	H-bond	R_{X-H}	ΔR_{X-H}	$R_{H...Y}$	$\delta R_{H...Y}$	<X-H…Y
PRM.3H2O	C1-H3…O42	1.089	-0.01	2.502	0.398	156.4
	C6-H8…O11	1.089	0	2.341	0.559	102.6
	C28-H31…N16	1.088	0	2.311	0.042	102.8
	C32-H33…N18	1.097	0.009	2.858	0.808	70.5
	C28-H30…N19	1.096	0	2.092	0.781	40.9
	C28-H29…N19	1.100	0.002	2.119	0.796	37.7
	C32-H34…N19	1.092	-0.009	2.104	0.821	40.7
	O36-H38…N5	0.969	0	4.032	0.743	81.5
	O39-H41…C12	0.971	0.002	2.063	0.657	165.7
	C24-H25…O39	1.098	0.006	2.545	0.355	53.2
	C6-H7…O42	1.094	-0.005	2.516	0.384	152.7
PRM	C1-H3	1.099				
	C6-H7	1.099				
	C6-H8	1.089				
	C28-H31	1.088				
	C32-H33	1.088				
	C28-H29	1.098				
	C32-H34	1.101				
	C24-H25	1.092				
H2O	O-H	0.969				

In PRM , the bond length of C_6-H_8 in methyl group 2 decreases while comparing with other methyl groups , which indicates the presence of C_6-H_8...O_{11} hydrogen bonding. Similarly, C_1-H_4 bond length in methyl group 1 is decreased due to the presence of C_1-H_4...O_{12} hydrogen bonding . The C-N bond length N_{16}-C_{17} (1.350) is increased due to the presence of weak intermolecular hydrogen bonding C_{28}-H_{31}...N_{16}. The existence of methyl group 5 and 6 provide the additional negative charge to the amino nitrogen atom resulting the contraction of bond length C_{17}-N_{19}. Comparing with other three compounds the C_{15}-C_{20} bond length increases due to steric hindrance of H_{23}…H_{26} (2.518). The bond length of C_{14}-C_{13} increases when compared with other three compounds shows the substitution of methyl group 4. The dihedral angle C_{10}-O_{12}-C_{13}-C_{14} shows the crabamate group is non-planar with the pyrimidine ring . N_{18}-C_{17}-N_{19}-C_{32} and N_{16}-C_{17}-N_{19}-C_{28} (-1.7^0 and 6.8^0) showing that the dimethyl amino group in nonplanar with the pyrimidine ring. Thus the compound pyrimidine is nonplanar in nature.

In PRM.3H_2O the C_1-H_3 bond length increased (0.004A^0) increased due to C_1-H_2…O_{42} hydrogen bonding interaction. In PRM.3H_2O complex C_6-H_7 bond length is increased when compared with PRM due to the influence of C_7-H_8…O_{42}^w hydrogen bonding interaction. Due to C_{32}-H_{34}…N_{19}^w hydrogen bonding interaction the C_{32}-C_{34} bond length is decreased in PRM.3H_2O complex compared with PRM.

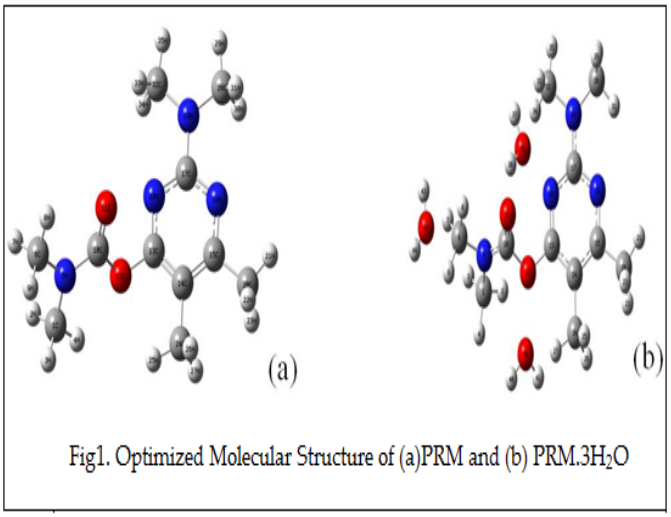

Fig1. Optimized Molecular Structure of (a)PRM and (b) PRM.3H_2O

3.2 VIBRATIONAL FREQUENCIES

The harmonic vibrational wave numbers and their shifts calculated at the B3LYP/6-31G(d) level listed in table 2. The red shift in the X-H stretching vibrational frequency has been widely used important intermolecular hydrogen bonding interaction. A shift to lower frequency relative to reference state is called a red shift. Contrarily, a shift to higher frequency is called a blue shift [6]. The larger shift value indicates the stronger H-bond interactions. The shifting of X-H stretching vibrational modes mix with other vibrational modes.

Table 2: THE VIBRATIONAL WAVE NUMBER OF PRM and PRM.3H_2O COMPLEX CORRESPONDING HYDROGEN BONDS

Compound	H-bond	υX-H	Δυ(X-H)
	C1-H3…O42^W	$3063_{(asy)}$	10
		$2939_{(sy)}$	29
PRM.3H2O	C6-H8…O11	$3073_{(asy)}$	2
		$2924_{(sy)}$	6
	C32-H33…N18	$3027_{(asy)}$	-44
		$2930_{(sy)}$	29
	C28-H29…N19	$3072_{(asy)}$	-4
		$2907_{(sy)}$	-3
	O36-H37^W…N18	$3662_{(asy)}$	-39
		$3526_{(sy)}$	-60
	O39-H41^W…C12	$3678_{(asy)}$	-23
		$3571_{(sy)}$	-15
	C24-H25…O39^W	$3052_{(asy)}$	17
		2923	4
	C1-H3	$3053_{(asy)}$	
		$2910_{(sy)}$	
PRM	C6-H8	$3071_{(asy)}$	
		$2918_{(sy)}$	
	C32-H33	$3071_{(asy)}$	
		$2901_{(sy)}$	
	C28-H29	$3076_{(asy)}$	
		$2910_{(sy)}$	
	C24-H25	$3035_{(asy)}$	
		$2919_{(sy)}$	
	OH	$3701_{(asy)}$	
H2O		$3586_{(sy)}$	

The intramolecular C_8-H_{15}…N_{18} hydrogen bonding interaction in PRM leads to the mixture of C-H stretching with pyrimidine ring stretching modes. In PRM.3H_2O complex the $\Delta\upsilon_{X\text{-}H}$ value of intermolecular hydrogen bonding interaction red shifted about 44 cm^{-1} due to the strong O_{36}-H_{37}…N^{18} intermolecular hydrogen bonding interaction. The C_1-H_3…O_{11} hydrogen bonding interaction have blue shifted about 10 cm^{-1}. In other red shifted hydrogen bonding interaction are C_{28}-H_{29}…N_{19}, O_{36}-H_{37}…N_{18} andO_{39}-H_{41}…C_{12} was supported by NBO and structural analysis.

3.3 NATURAL BOND ANALYSIS

The natural bond orbitals (NBO) calculations were performed using NBO 3.1 program as implemented in the Gaussian 09 package at the B3LYP 631-G(d) level in order to understand various second-order interactions between the filled orbitals of one subsystem and vacant orbitals of another subsystem, which is a measure of the intramolecular delocalization or hyper conjugation.

The second-order Fock-matrix was carried out to evaluate the donor-acceptor interactions in the NBO basis . The interactions result in a loss of occupancy from the localized NBO of the idealized Lewis structure into an empty non-Lewis orbital. For each donor (i) and acceptor (j) the stabilization energy $E^{(2)}$ associated with the delocalization $i \rightarrow j$ is determined as

$$E^{(2)} = \Delta E_{ij} = q_i \frac{F_{ij}^2}{(E_i - E_j)}$$

where, q_i - donor orbital occupancy

E_i, E_j - diagonal elements

F_{ij} - the off diagonal NBO Fock matrix element.

NBO analysis provides the most accurate possible 'natural Lewis structure' picture of 'j' because all orbital details are mathematically chosen to include the highest possible percentage of the electron density. A useful aspect of the NBO method is that it gives information about interactions of both filled and virtual orbital spaces that could enhance the analysis of intra and inter molecular interactions. The electron density of conjugated single as well as double bond of pyrimidine ring about 1.976 - 1.987e clearly demonstrate strong delocalization for Pirimor. The intermolecular interaction are formed by the orbital overlap between σ(N-C)→σ*(O-C), σ(C-C)→σ*(C-C)σ(C-N)→σ*(C-N) and σ(C-N)→σ*(N-C) bond orbital which orbital which results intramolecular charge transfer (ICT) causing stabilization of the system as seen from the table 3. The stabilization energy contributions from the σ(C_{13}-C_{14})→σ*(C_{10}-O_{12}) interaction is 8.24kJ/mol. The hydrogen bonding interaction between the oxygen cone pair and (C-H) antibonding.ie, σ (O_{11})→σ*(C_6-H_8) increases the C_6-H_8 bond.

TABLE 3: SECOND ORDER PERTURBATION THEORY ANALYSIS OF FOCK MATRIX IN NBO BASIS CORRESPONDING TO THE INTRA MOLECULAR HYDROGEN BONDS AND HYPERCONJUGATION IN PRM AND PRM.3H_2O COMPLEX INTRACTION ENERGIES (E2) IN KJ MOL^{-1} WITH HYBRID ORBITALS AND ELECTRON DENSITY(E.D)

Complex	H-bond	RX-H	ΔRX-H	RH...Y	δRH…Y
PRM. 3H2O	C1-H3…O42	1.089	-0.01	2.502	980
	C6-H8…O11	1.089	0	2.341	0.559
	C28-H31…N16	1.088	0	2.311	0.042
	C32-H33…N18	1.097	0.009	2.858	0.808
	C28-H30…N19	1.096	0	2.092	0.781
	C28-H29…N19	1.1	0.002	2.119	0.796
	C32-H34…N19	1.092	-0.009	2.104	0.821
	O36-H38…N5	0.969	0	4.032	0.743
	O39-H41…C12	0.971	0.002	2.063	0.657
	C24-H25…O39	1.098	0.006	2.545	0.355
	C6-H7…O42	1.094	-0.005	2.516	0.384
PRM	C1-H3	1.099			
	C6-H7	1.099			
	C6-H8	1.089			
	C28-H31	1.088			
	C32-H33	1.088			
	C28-H29	1.098			
	C32-H34	1.101			
	C24-H25	1.092			
H2O	O-H	0.969			

The shortening of C_6-H_8 is due to C-H…O hydrogen bonding having stabilization energy 4.184 KJ/mol. The existence of weak intermolecular C-H…O hydrogen bond due to interaction between lone pairs of σ (O_{12}) with (C_1-H_4) (26.359 kJ/mol) have confirmed. The corresponding intra-molecular H…O distance (H_8….O_{11})/ (H_4….O_{12}) is found to be 2.309 and 2.235Å. These distances are significantly shorten than that of Vander waals seperation between the oxygen atom and the hydrogen atom (2.720Å) indicating the existence of C-H...O interaction [7]. The interaction C-H...N hydrogen bonding between cone pairs (N_{16}) to antibonding σ*(C_{28}-H_{31}) (8.242 kJ/mol) have been confirmed by the results of NBO analysis.

3.4 CHARGE ANALYSIS

All hydrogen atoms have positive charge. Hydrogen in methyl group is more positive than hydrogen in ring. The largest positive charge occurs at H_{33} in PRM, which are involved in C_{32}-H_{33}…N_{18} hydrogen bonding with atomic charges of 0.263e.

TABLE 4: CHARGE ANALYSIS TABLE

Atom	Natural Charge	
	PRM	PRM.3H_2O
C1	-0.469	-0.464
H2	0.222	0.228
H3	0.219	0.229
H4	0.257	0.24
N5	-0.488	-0.489
C6	-0.469	-0.482
H7	0.22	0.222
H8	0.263	0.259
H9	0.218	0.231
C10	0.948	0.935
O11	-0.631	-0.628
O12	-0.578	-0.585
C13	0.587	0.585
C14	-0.178	-0.176
C15	0.284	0.288
N16	-0.555	-0.551
C17	0.621	0.623
N18	-0.559	-0.573
N19	-0.436	-0.434
C20	-0.706	-0.707
H21	0.255	0.256
H22	0.245	0.246
H23	0.242	0.245
C24	-0.691	-0.679
H25	0.253	0.229
H26	0.24	0.243
H27	0.237	0.251
C28	-0.469	-0.469
H29	0.218	0.22
H30	0.213	0.214

H31	0.262	0.263
C32	-0.469	-0.459
H33	0.264	0.245
H34	0.212	0.216
H35	0.22	0.226

In PRM.3H_2O largest positive charge occurs at H_{31} due to C_{28}-H_{31}…N_{16} hydrogen bonding interaction. Charge of N_{18} is decreased by the influence of C_{25}-H_{26}…N_{18} hyperconjugative interaction. It is worthy to mention that C_{10}, C_{13}, C_{17} and C_{15} atoms exhibit positive charge while other carbon atoms exhibit negative charge. The more negative values on C_{20} and C_{24} of CH_3 group leads to a redistribution of electron density and also influenced by H_{23}…H_{27} steric repulsion. The negative charges located at atoms O_{11} and O_{12} will interact with C_{10} and C_{13} atoms due to inductive effect the bond distance N_5-C_{10} (1.364A˚) increases. The presence of two large electronegative oxygn atom and one nitrogen atom impose very high charge on carbon atom (C_{10}) in the carbamate group.

3.5 HIRSHFELD SURFACE ANALYSIS

The Hirshfeld surface analysis, a unique new method of visualizing the intra molecular interaction, was performed in order to explore the properties of all inter contacts within the crystal structure of PRM. Additionally corresponding two-dimensional (2-D) fingerprint plots [8] provide rapid quantitative summary of them (the percentage of each contact), which is important for understanding of the contribution of intra molecular interactions to the crystal packing. This plot provides information not only about close contacts, but also about more distant contacts and areas where the interactions are the weakest. Hirshfeld surface display all of the inter contacts within the crystal at once and are therefore ideal for analyzing the crystal packing. The molecular Hirshfeld surface were constructed on both d_e (external distance that is the distance between the Hirshfeld Surface and the nearest atom of an adjacent molecule.), d_i (internal distance that is the distance from the nearest nucleus internal to the calculated Hirshfeld surface and the vanderWaals radii of the atom, enabling identification based on the electron distribution calculated as the sum of spherical atom electron densities [9].The Hirshfeld surfaces of PRM crystal structure have been mapped over. The d_e 1.000 to 2.650 A^0, the d_i is 0.961 to 2.650 A^0, d_{norm} is -0.271 to 1.226 A^0 for PRM. Fig represents the d_{norm}, d_i, d_e, shape index and curvedness of PRM. The shape index and curvedness surfaces have been shown to give the information about each donor-acceptor pair and to measure how much effectively divides the surfaces into set of patches respectively.is shown in fig 2. Fingerprint plots give an idea about interactions with in the molecule.

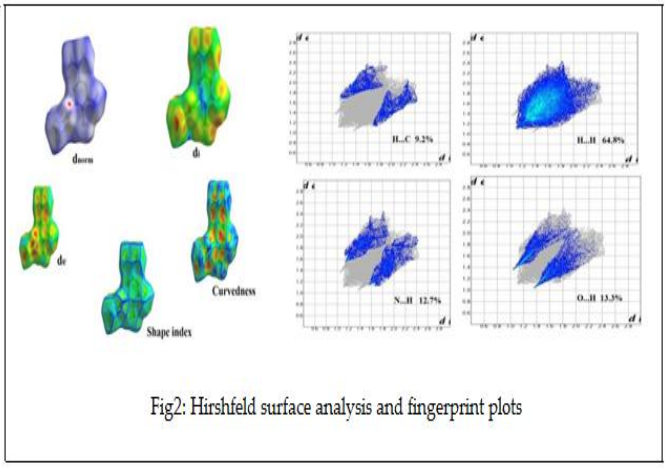

Fig2: Hirshfeld surface analysis and fingerprint plots

3.6 HOMO LUMO ANALYSIS

According to the frontier molecular orbital theory (FMO) of chemical reactivity, transition of electron is due to interaction between highest occupied molecular orbital (HOMO) and lowest unoccupied molecular orbital (LUMO) of reacting species [10]. E_{HOMO} is a quantum chemical parameter which is often associated with the electron donating ability of the molecule. High value of E_{HOMO} is likely to a tendency of the molecule to donate electrons to appropriate acceptor molecule of low empty molecular orbital energy [11].

The molecule interacts with other species; hence, they are called the Frontier molecular orbitals (FMO's). HOMO, which can be thought the outermost orbital containing electrons, tends to act as electron donor. On the other hand, LUMO can be thought the innermost orbital containing free places to accept electrons. To explain several types of reactions and for predicting the most reactive position in conjugated systems, molecular orbital and their properties are used. A molecule having a small frontier orbital gap is more polarizable and is generally associated with a high chemical reactivity and low kinetic stability [12]

The plots of MO's (HOMO and LUMO) are shown in fig.3 and its energy values are given in table 5. All the HOMO and LUMO have nodes. The nodes in each HOMO and LUMO are placed symmetrically. The positive phase is red and the negative is green. In the title compound, the HOMO is delocalized over the carbamate group. By contrast, the LUMO is located over the dimethyl amino pyrimidine.

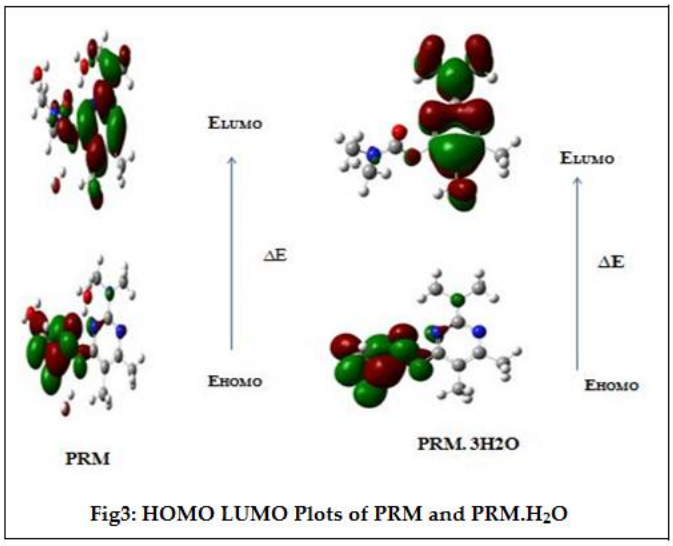

Fig3: HOMO LUMO Plots of PRM and PRM.H_2O

Global Reactivity Descriptors

By using HOMO and LUMO energy values of a molecule, the global chemical reactivity descriptor of molecules such as hardness, chemical potential, softness, electronegativity and electrophilicity index as well as local reactivity have been defined [13]. The HOMO and LUMO energies, the energy gap (E), ionization potential (I), electron affinity (A), absolute electronegativity (χ) absolute hardness (η),and softness of title compound and its related compounds computed by DFT/B3LYP/6-31G(d) level.

The chemical potential provide a global reactivity index and related to charge transfer from a system of higher chemical potential to lower chemical potential. The reactivity index is the measure of stabilization in energy when the system acquires an additional electronic charge (N). A molecule or atom that has a positive electron affinity is often called an electron acceptor and may undergo charge transfer reactions. The electron donating power of a donor molecule is measured by its ionization potential which is the energy required to remove an electron from the highest occupied molecular orbital. The overall energy balance (ΔE), i.e., energy gained or lost, in an electron donor acceptor transfer is determined by the difference between the acceptor's electron affinity (EA) and the ionization potential (IP) as ΔE=EA-IP. Electronegativity is a chemical property that describes the ability of an atom or a functional group to attract electrons or electron density towards itself. Parr et al. have proposed electrophilicity index (ω) as a measure of energy lowering due to maximal electron flow between donor and acceptor [14]. The usefulness of this new reactivity quantity has been recently demonstrated understanding the toxicity of various pollutants in terms of their reactivity and site selectivity. The electrophilicity index is positive, definite quantity and direction of the charge transfer is fully determined by the chemical potential (V) of the molecule. Because an electrophile is a chemical species, it has an electron accepting capability from the environment and its energy must decrease upon accepting electronic charge, therefore, its electronic chemical potential must be negative. Using Koopman's theorem for closed shell compounds the electronegativity and chemical hardness can be calculated as follows:

$$\text{Electronegativity}, \chi = -\frac{1}{2}(E_{LUMO} + E_{HOMO})$$

$$\text{Chemical reactivity}, \boldsymbol{\eta} = \frac{1}{2}(E_{LUMO} - E_{HOMO})$$

Softness, $\sigma=1/\eta$

Electrophilicity index, $\omega = \mu^2 / 2\eta$

where I and A are Ionisation Potential and Electron Affinity. Large HOMO-LUMO gap means a hard molecule and small HOMO-LUMO gap means a soft molecule. One can also relate the stability of the molecule to hardness, which means that the molecule with least HOMO-LUMO gap means it is more reactive.

The usefulness of this new reactivity quantitivity has been recently demonstrated in understanding the toxicity of various pollutants in terms of their reactivity and site selectivity [15]. The calculated parameters are shown in Table.5. Global softness 0.271 shows more chemical active nature of PRM, and electrophilicity index 11.744, which shows more bio active nature of PRM.3H_2O complex while comparing with PRM while comparing with PRM.3H_2O.

TABLE 5: CALCULATED GLOBAL PARAMETERS

	PRM	PRM.3H_2O
Ionization Potential (I)	8.453	8.42
Electron Affinity (A)	4.705	4.736
Electro negativity (χ)	-6.579	-6.578
Chemical potential (η)	6.579	6.578
Hardness	1.874	1.842
Softness	0.267	0.271
electrophilicity index (ω)	11.547	11.744

CONCLUSION

The present study has been performed on Pirimor its water complex (PRM.3H_2O) to investigate the intermolecular hydrogen bonding interaction to show the insecticidal activity. The theoretically predicted optimized geometry of Pirimor and its related compounds by DFT method suggests the possibility of intermolecular C-H...O and C-H...N hydrogen bonding. The stretching vibration of dimethyl amino group shows a blue shift due to the C-H...N hydrogen bonding. The lowering of Homo-Lumo energy gap of Pirimor while compairing with PRM.3H_2O indicate the charge transfer. The carbon atom in carbamate group (C_{10}) shows more positive charge which shows charge transfer from carbamate to dimethyl amino pyrimidine group. NBO analysis confirms the possibility of C-H...O and C-H...N hydrogen bonding. The experimental and theoretical vibarational, NBO, HOMO-LUMO energy gap, global softness and electrophilicity index shows more insecticidal activity of PRM.3H2O in comparison with Pirimor compound.

REFERENCES

[1] V. Balachandran, A. Lakshmi, A. Janaki, Spectrochimica Acta Part A: Molecular and Biomolecular Spectroscopy, 81 (2011) 1-7.

[2] Mariana Rocha, Alejandro Di Santo, Juan Marcelo Arias, Diego M. Gil,Aída Ben Altabef, Spectrochimica Acta Part A: Molecular and Biomolecular Spectroscopy, S1386-1425(14)01435-8doi:10.1016/j.saa.2014.09.077.

[3] M.Amalanathan, I.Hubrt Joe,V.K.Rastogi, Journal of Molecular Structure 985(2011) 48-56.

[4] Rong Zhang, Haoran Li, Yi Lei, Shijun Han, Journal of Molecular Structure 693 (2004) 17–25.

[5] Hojin Yang,Tae Ho Kim, Yong Woon ShinKi-Min, Park and Jineun Kim, Acta Cryst. (2010). E66, o1998.

[6] P. Hobza, Z. Havlas, Chem. Rev. 100 (2000) 4253.

[7] V.Santhana Krishnan,S.Sampath Krishnan,S.Muthu, Spectrochimica Acta Part A: Molecular and Biomolecular Spectroscopy 115 (2013) 191–201.

[8] Jack D.Dunitz, Angelo Gavezzotti, Chem.Soc.Rev. 2009,38,2622-2633.

[9] Saikat Kumar Singh, Journal of molecular structure 1064 (2014) 70-75.

[10] C.Ravikumar,L.Padmaja,I.Hubert Joe, Spectrochimica Acta Part A 75(2010) 859-866.

[11] Lynnette Joseph,D.Sajan,K.Chaitanya, Jayakumary Isac, Spectrochimica Acta Part A: Molecular and Biomolecular Spectroscopy 122(2014)375-380.

[12] A.Natraj,V.Balachandran,T.Karthick, Journal of molecular structure 1022 (2012)94-108.

[13] Wajdi.M.Zoghaib,John Husband,Usama A.Soliman, Ibrahim A Shaaban, Tarek A.Mohemed, Spectrochimica Acta Part A: Molecular and Biomolecular Spectroscopy 105(2013) 446-455.

[14] Sameh Guidara, Habib Feki, Younes Abid, , Spectrochimica Acta Part A: Molecular and Biomolecular Spectroscopy 133 (2014) 856-866.

[15] D. Arul Dhas; I. Hubert Joe; S.D.D. Roy; S. Balachandran, Spectrochimica Acta Part A 79 (2011) 993– 1003. 10.1016/j.saa.2011.04.011.